Simulation of geological graphene genesis by the piston-cylinder apparatus

Simulação da gênese de grafeno geológico por aparato pistão-cilindro

Augusto Gonçalves Nobre[1, 2] ⬤, Andrés Fabián Salazar-Naranjo[1] ⬤, Fabio Ramos Dias de Andrade[1] ⬤,
Silvio Roberto Farias Vlach[1] ⬤, Rômulo Augusto Ando[3] ⬤

[1]Universidade de São Paulo, Instituto de Geociências. Rua do Lago, 562, Butantã, 05508-080, São Paulo, SP, Brasil.
[2]Universidade Federal de Pelotas, Instituto de Ciências Humanas. Alameda Barroso, 1202, Centro, 96010-280, Pelotas, RS, Brasil.
[3]Universidade de São Paulo, Instituto de Química. Av. Prof. Lineu Prestes, 748, Butantã, 05508-900, São Paulo, SP, Brasil.
e-mail: augusto.goncalves@usp.br; andres.salazar@usp.br; dias@usp.br; srfvlach@usp.br, raando@iq.usp.br

ABSTRACT

Stable natural graphene occurs in graphite- and phyllosilicate-bearing low-grade metamorphic rocks. The present work simulates the process of geological formation of graphene using a piston-cylinder apparatus, promoting diffusion between talc and graphite at 700ºC and 900 MPa for a period of 24 h. The experimental products were analyzed by optical and scanning electron microscopy for description of the microstructures formed between the mineral precursors. The talc-graphite diffusion zone was also analyzed by Raman spectroscopy. Results indicate that graphite becomes progressively more deformed near the talc diffusion zone and eventually undergoes cleavage. Graphene becomes stable on the talc substrate in the center of diffusion zone. Therefore, the search for deposits of natural graphene and other nanomaterials in geological context is promising.

Keywords: Mineral nanotechnology; Natural graphene; Experimental mineralogy; Graphite; Talc.

1. INTRODUCTION

Examples of mineral nanotechnology processes that provide graphene and its derivative compounds (such as graphene oxide and reduced graphene oxide) using mineral raw materials have been reported in the literature over the last decade [1–4]. Mineral nanotechnology is an emerging area between Geology and Materials Sciences aiming for (i) increasing the quality of mineral supplies to produce nanomaterials and (ii) the direct exploration of natural nanometric minerals that already behave as nanomaterials for industrial uses. Mineral nanotechnology approaches nanomaterials production by top-down techniques, avoiding synthesis processes and focusing on the materials properties and applications, seeking to comply with the best circular economy and environmental initiatives [5, 6].

A prominent example of mineral nanotechnology is obtaining graphene from natural graphite. The area of graphene geology may be subdivided in (i) the production of graphene devices from mineral graphite [7, 8] and (ii) the extraction of graphite nanoplatelets and graphene directly from geological deposits [9]. Although minerals have impurities and crystalline defects, recent studies [10, 11] have shown that geological environments are able to provide two-dimensional natural minerals, which may replace synthetic bidimensional materials in some cases.

Due to its two-dimensional structure and its physical and chemical properties, graphene has become a potential exponent of nanotechnology [12, 13]. Nanostructured devices are considered the key to solving the problems encountered in the implementation and popularization of enabling technologies of the Fourth Industrial Revolution, providing hitherto unprecedented physical and chemical properties by new nanomaterials, such as graphene, which can lead to relevant advances in the most diverse areas of science, such as telecommunications and information technology [14, 15].

The natural formation of graphene requires a suitable rock in terms of mineral composition and structure, which has to be submitted to deformation under thermodynamic conditions that allow the systematic cleavage of graphite in contact with other placoid minerals that act as a substrate to stabilize the graphene. As reported in

the literature [16, 17], the most favorable minerals as a substrate for cleaved graphite are the phyllosilicates, due to the crystallographic affinity in the parallel to the crystallographic c-axis with graphite and important presence of van der Waals forces in their crystalline structure [18, 19].

An example of natural occurrence of graphene is in a metamorphic belt in sourthern Brazil, where dolomitic rocks underwent metamorphism, shearing and reaction with silica-bearing fluids, hydrothermalism, leading to the formation of talc deposits. The conditions of metamorphism were at least 200 MPa and 570ºC, an event that took place 630 million years ago [20–22]. Graphene was formed by graphite cleavage and stabilized in the surface of talc, where it still stable until today.

The end-loaded piston-cylinder apparatus [23] is designed to simulate pressure and temperature conditions existing in Earth's interior. This equipment is traditionally used in experimental petrology to study relations of phase equilibrium, melting and crystallization of geological materials [24]. In the present work, a piston-cylinder equipment is used to simulate the geological conditions that isolate and stabilize natural graphene. Constraining the key parameters in graphite formation and stabilization in natural environments is of fundamental importance in the prospection of natural graphene deposits.

2. MATERIALS AND METHODS

The studies were carried out with an end-loaded Bristol-type piston-cylinder apparatus (Figure 1) at the Experimental Petrology and Geochemistry Lab at the Institute of Geosciences of the University of Sao Paulo (IGc-USP). The temperature was set up and monitored using a B-type thermocouple and a 2404 Eurotherm PID controller.

2.1. Sample preparation for piston-cylinder apparatus

The starting materials were 2 mm long, 2.6 mm diameter, billets of synthetic pure graphite and natural talc (containing some quartz and clinochlore minor contaminants). They were placed in contact to allow mutual diffusion inside a sample holder of high melting point and chemical stability composed by 6 mm long $Au_{75}Pd_{25}$ alloy tube welded at the base, slightly compressed, and weld-close, as a trash-can type experimental capsule. The capsule was loaded into a 3/4" furnace assembly that contained the reactants (starting sample) was formed concentric layers composed by crushable MgO which acts as a sample holder fixer, graphite heater, pyrex (B-silicate) glass (spacer) and NaCl sleeves to maintain the almost friction-free sample [25], besides steel plugs (Figure 2). The system assembly of the piston-cylinder apparatus complies with VLACH *et al.* [26] procedures. An alumina two-bore insulator allows thermocouple insertion and temperature measures on the capsule top-end, isolated from the thermocouple probe with a thin Al disk.
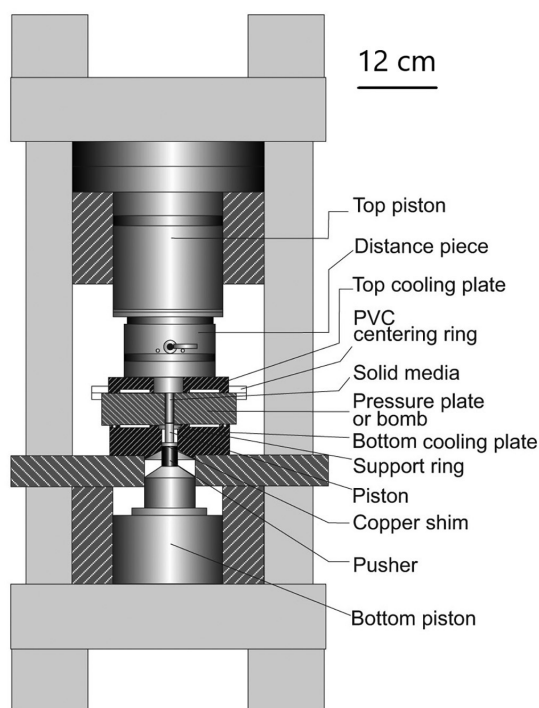
Figure 1: Schematic representation of the main core of the Bristol-type end-loaded piston-cylinder (200 tons).
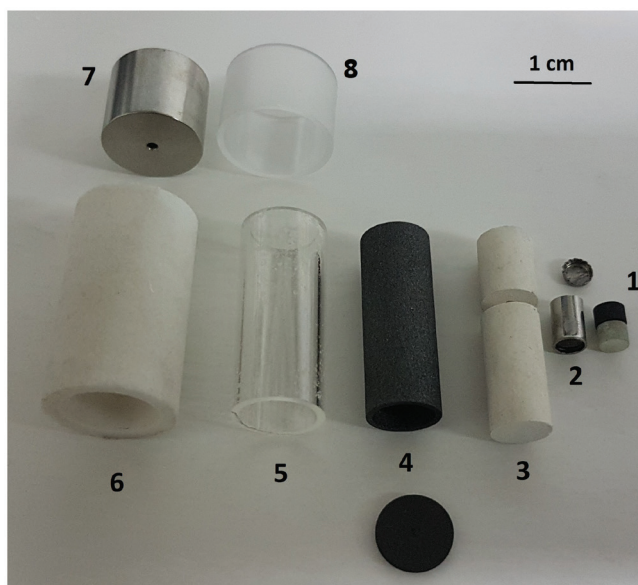
Figure 2: Furnace assembly for piston- cylinder. 1: Talc (green) and graphite (black) in billets; 2: Sample holder; 3: Upper and Lower crushable MgO; 4: Graphite heater with lid; 5: Pyrex glass spacer; 6: NaCl sleeve; 7: Steel plug; 8: Pyrex glass insulator. Sample capsule is placed in the internal, centralized, upper part of the Lower MgO component. Note bores for thermocouple accommodation in both the upper MgO and Steel plug.

The piston-cylinder simulates approximately lithostatic pressure (equal in all directions), in which the uniaxial pressure generated by the piston is uniformly distributed on the experimental assembly within the pressure plate (Figure 1). This way of applying pressure is different from the shear tectonic movements especially favorable to the cleavage of minerals formed by van der Waals interactions. In this way, this study was able to evaluate more conservative conditions for the emergence of geological graphene.

2.2. Definition of pressure and temperature conditions for test conduction

It is not possible to simulate the geological time scale in the laboratory, in the magnitude of millions of years, therefore experimental conditions were chosen at the highest possible temperature and pressure in which both talc and graphite are stable, in order to accelerate the process of graphene formation in 24 hours long experiments. The experiment was conducted at a temperature of 700°C so there is no thermal decomposition of talc ($Mg_3Si_4O_{10}(OH)_2$) into enstatite ($MgSiO_3$), silica (SiO_2), and water (H_2O) at the experiment pressure, as can be seen in the Equation 1 [27]. The pressure of 900 MPa is below pressure of graphite phase change to lonsdaleite, also known as h-diamond [28] under the temperature conditions of the experiment. After the desired time, the equipment power was cut off and the experimental assembly was quenched to the room temperature at an approximate rate of –30°C/s. The cooling rate represents the rate available in the equipment, quickly enough to avoid phases re-equilibrium, preserving the microstructures formed during the thermal treatment.

$$Mg_3SiO_{10}(OH)_2 \rightarrow 3MgSiO_3 + SiO_2 + H_2O$$

(1)
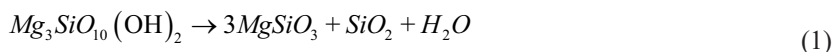
These parameters ensured that the mineral precursors remained stable throughout the experiment, allowing the predominant process to be diffusion, consequently allowing efficient cleavage between the minerals.

2.3. Sample characterization

After the experiment, the welded AuPd capsule containing the sample was longitudinally sawn and was fixed in epoxy resin to allow manipulation and characterization.

Diffusion in the contact between the graphite and talc was observed with reflected light optical microscopy (RLOM, Zeiss Axio Imager, equipped with the Zeiss AxioCam system) and scanning electron microscopy (SEM, LEO 440I) with secondary (SE) and compositional mode of backscattered electrons (BSE). The SEM analytical conditions were 20 kV voltage, working distance of 25 mm and sample current between 600 and 1200 pA.

Graphite-talc diffusion zones were studied by Raman spectroscopy using a WITec Raman microscope alpha 300 R with a 633 nm excitation laser, with 10 accumulations in an integration time of 2 s at the Molecular Spectroscopy Laboratory (LEM) at the Institute of Chemistry of the University of São Paulo (IQ-USP).

Characterization by Raman spectroscopy considered the relative intensity between the D (approximately 1350 cm^{-1} – corresponding to defects in covalent bonds), G (approximately 1580 cm^{-1} – associated with the sp^2 carbon atoms plane vibration), and 2D (approximately 2700 cm^{-1} – linked to structural arrangement of the two-dimensional plane) of graphite-graphene spectral bands system [29–32]. The spectra were acquired from in-line profiling to allow the observation of the spectra variation perpendicularly to the diffusion zone.

## 3. RESULTS AND DISCUSSION

3.1. Microscopy

In all micrographs obtained by RLOM and SEM (Figure 3) graphite is in the upper and talc in the lower portion. The Figure 3(a) shows the longitudinal section of the AuPd alloy capsule with the graphite and talc zones. Microstructural differences in the mineral precursors are shown in Figure 3(b). Graphite flakes display well-marked grain boundaries and can be classified as tabular vanes with polygonal basal section. Talc crystals are not distinguishable in the micrographs, given the material rheological behavior 23, which is extremely moldable, even under room conditions.

The talc zone in shown by BSE in Figure 3(c), highlighting fractures and other general imperfections formed in this sample region.

Polygonized graphite crystals and the mass of indistinguishable talc crystals with rough surface are shown in Figure 3(d) (SE), with a thickness between 5 and 20 μm in the diffusion zone.

The average atomic number difference between talc (highest), graphite (intermediate) and diffusion (lowest) zones are differentiable in the BSE image in Figure 3(e). It is possible to observe the difference in morphology formed between the diffusion (with lower topography), graphite (granular crystals with intermediate topography) and talc zones (higher topography) in the SE image in Figure 3(f).

After experiment, the graphite preserves its even distribution of porosity, while talc has lower porosity and fractures. In the talc zone, it is still possible to observe the surface roughness generated by the small crystals aggregate.
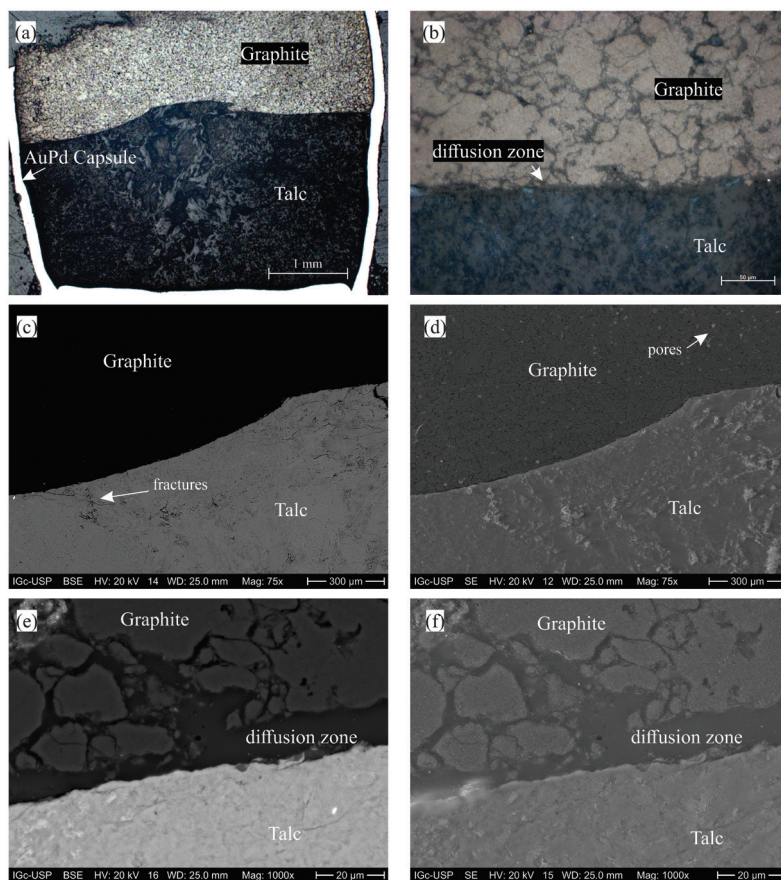
Figure 3: Sample photomicrographs. (a): RLOM – Sample holder capsule with talc and graphic zones. (b): RLOM – Talc, diffusion, and graphite zones. (c): BSE-SEM – Talc zone microstructure. (d): SE-SEM – Morfology of talc and graphite zones. (e): BSE-SEM – Average molar mass difference between talc, graphite, and diffusion zones. (f): SE-SEM – Morfology of talc, graphite, and diffusion zones.

The thickness of the diffusion zone is variable in the range of few tens of micrometers. It is characterized by low relief and lower average atomic number than that observed in the talc and graphite zones, which is a good indication of the efficient cleavage of both mineral phases.

3.2. Raman spectroscopy

The result of the in-line profiling analysis by Raman spectroscopy is shown in Figure 4. The guide points from where the spectra were acquired can be seen in Figure 4(a).

The Raman logging started in the graphite outside the diffusion zone (Figure 4(b), spectrum I). The Raman spectrum has an important D band intensity [33, 34], as in all natural graphites, but in this sample region the G band has significantly higher relative intensity.

Closer to the diffusion zone (Figure 4(b), spectrum II), intensity of G and D bands become similar, with a slightly higher G band.

This difference between the bands is inverted in the vicinity of the contact between talc and graphite (Figure 4(b), spectrum III), where D band has higher intensity than the G band.

At the boundary between the graphitic and diffusion zones (Figure 4(b), spectrum IV) graphite is intensely deformed, as the D band is much more intense than the G band.

The zone where graphite diffuses into talc (Figure 4(c), spectrum V) is marked by the presence of a talc with approximately 700 cm^{-1} diagnostic band associated with the bending modes of the Si-O-Si bridges [35], in addition to graphite with D band more intense that the G band.

Graphene is identified in the core of the diffusion region (Figure 4(c), spectrum VI), in which it is possible to observe the 2D band significantly more intense than the G band, in addition to the band of approximately 400 cm^{-1}, a segment of the spectrum linked to the lattice mode involving Mg-O bonds and the tetrahedral bending of talc structure.

In the diffusion zone closest to talc (Figure 4(c), spectrum VII) it is possible to identify the diagnostic bands of a deformed graphite with significant D intensity and the approximately 700 cm^{-1} and 1000 cm^{-1} bands of talc, respectively associated with the bending and stretching modes of the talc Si-O-Si bridges.

Finally, the talc zone (Figure 4(c), spectrum VIII) is characterized by bands of approximately 700 cm^{-1} and 1000 cm^{-1}, in addition to the region of approximately 300-600 cm^{-1} bands associated with lattice mode of Mg-O bonds and tetrahedral bending of the mineral.
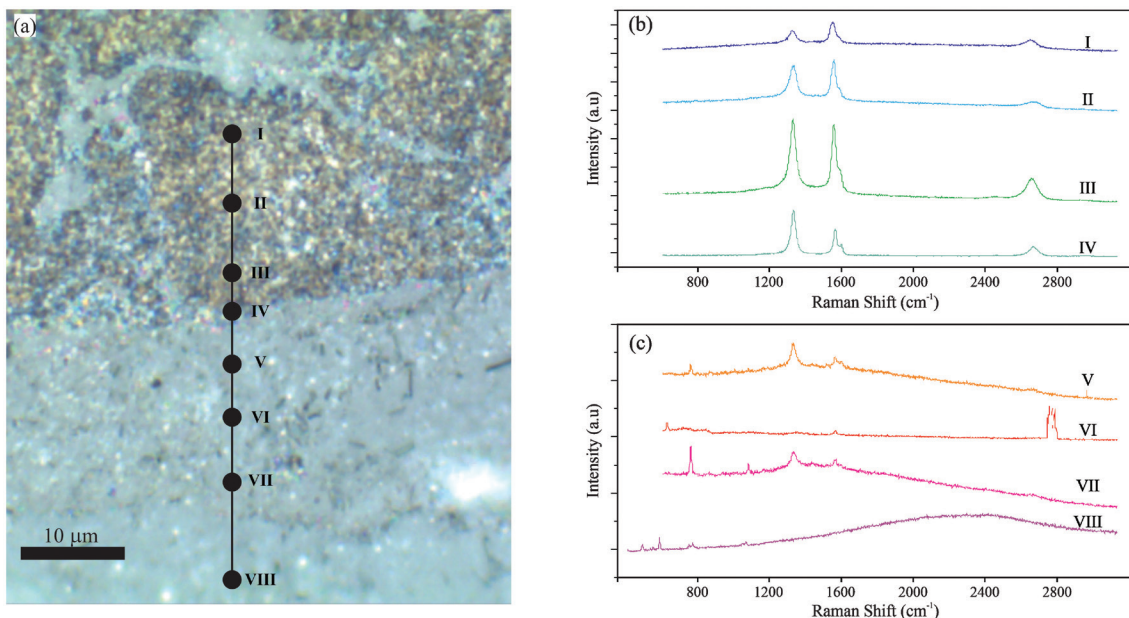
Figure 4: Results of in-line profiling Raman spectroscopy. (a): Micrograph with guide points for spectra acquisition. (b) Graphite zone spectra. I: Graphite zone – region without deformation generated by the diffusion process. II: Graphite zone – beginning of deformation by interference with the diffusion zone. III: Graphite zone – increased deformation caused by the diffusion zone. IV: Contact between graphite and diffusion zone, graphite strongly deformed. (c) Talc and diffusion zones spectra. V: Diffusion zone – presence of deformed graphite associated with talc. VI: Diffusion zone – graphene. VII: Diffusion zone – presence of talc associated with deformed graphite. VIII: Talc zone.

It is noteworthy that the graphite becomes progressively more deformed towards the diffusion zone. The diffusion zone is a transition layer between deformed graphite and talc with its core being the stabilizing graphene region.

4. CONCLUSIONS

Our results confirmed that it is possible to form and stabilize natural graphene in metamorphic rocks that have an adequate mineralogy, with appropriate contact between the mineral precursors and thermodynamic conditions favorable to the cleavage and anchoring of the formed bidimensional phase.

The mineralogy must have graphite, as the source of graphene, and another mineral with van der Waals forces that can interdigitate with graphite and serve as graphene substrate. The contact area between the mineral precursors should be as large as possible so that the diffusion zone, where the graphene stabilizes, is as wide as possible.

The piston-cylinder experiments demonstrated that graphene may be formed and stabilized in talc under approximately isostatic pressures and temperatures compatible with metamorphic processes inside the Earth's crust. It is expected that directional strain and the presence of hydrothermal fluids would favour the cleavage of minerals such as graphite and talc and therefore enhance graphene formation. Conditions of low oxygen fugacity are important as well, to avoid oxidation of carbon.

The experimental studies have shown that graphene can form under crustal pressure and temperature conditions corroborating its previous detection in metamorphic rocks. Formation graphene in nature is based on widely available minerals, exposed to ubiquitous metamorphic belts conditions in the continental crust. Hence, the search for geological settings favorable for graphene formation may lead to the discovery of significant deposits of this strategic nanomaterial.

5. ACKNOWLEDGMENTS

6. BIBLIOGRAPHY

[1] RODRIGUES, F.C., NOBRE, A.G., SILVA, E.E., *et al.*, "Graphite/metal electrodes for electrochemical exfoliation: few layers graphene with low defects", *Defect and Diffusion Forum*, v. 371, pp. 131–134, 2017. doi: http://dx.doi.org/10.4028/www.scientific.net/DDF.371.131.

[2] SIMÓN, M., BENÍTEZ, A., CABALLERO, A., *et al.*, "Untreated natural graphite as a graphene source for high-performance li-ion batteries", *Batteries*, v. 4, n. 1, pp. 13, 2018. doi: http://dx.doi.org/10.3390/batteries4010013.

[3] HOU, D., LI, K., MA, R., *et al.*, "Influence of order degree of coaly graphite on its structure change during preparation of graphene oxide", *Journal of Materiomics*, v. 6, n. 3, pp. 626–641, 2020. doi: http://dx.doi.org/10.1016/j.jmat.2020.04.009.

[4] MARTINEZ, J.A.E., SANCHEZ-JUNIOR, M., GONÇALVES, A.N., *et al.*, "Influence of different oxidation mechanisms on the exfoliation of intercalated graphite bisulfate using two types of graphite", *Matéria (Rio de Janeiro)*, v. 26, n. 2, pp. e12993, 2021. doi: http://dx.doi.org/10.1590/s1517-707620210002.1293.

[5] NOBRE, A.G., MARTINEZ, J.A.E., FLORENCIO, O., "Mineral nanotechnology in circular economy", In: Iano, Y., Saotome, O., Kemper, G., Mendes de Seixas, A.C., Gomes de Oliveira, G. (eds), Smart Innovation, Systems and Technologies, 1 ed., chapter 26, Cham, Switzerland, Springer Nature, 2021. doi: https://doi.org/10.1007/978-3-030-75680-2_26.

[6] HOCHELLA JUNIOR, M.F., LOWER, S.K., MAURICE, P.A., *et al.*, "Mineral nanoparticles and earth systems", *Science*, v. 319, n. 5870, pp. 1631–1635, 2008. doi: http://dx.doi.org/10.1126/science.1141134. PubMed PMID: 18356515.

[7] AMBROSI, A., CHUA, C., KHERZI, B., *et al.*, "Chemically reduced graphene contains inherent metallic impurities present in parent natural and synthetic graphite", *Proceedings of the National Academy of Sciences of the United States of America*, v. 109, n. 32, pp. 12899–12904, 2012. doi: http://dx.doi.org/10.1073/pnas.1205388109. PubMed PMID: 22826262.

[8] WONG, C.H., SOFER, Z., PUMERA, M., "Geographical and geological origin of natural graphite heavily influence the electrical and electrochemical properties of chemically modified graphenes", *Chemistry (Weinheim an der Bergstrasse, Germany)*, v. 21, n. 23, pp. 8435–8440, 2015. doi: http://dx.doi.org/10.1002/chem.201500116. PubMed PMID: 25858504.

[9] NOBRE, A.G., MARTINEZ, J.A.E., TERENCE, M.C., *et al* ., "The action of shear zones in the natural availability of graphite nanoplatelets: the example of the metadolomites of the Itaiacoca Group and the mica schist of the Dom Silverio Group", *Brazilian Journal of Animal and Environmental Research*, v. 3, n. 4, pp. 3108–3118, 2020. http://dx.doi.org/10.34188/bjaerv3n4-031.

[10] NOBRE, A.G., ANDRADE, F.R.D., "Estudo de origem e caracterização nanotecnológica de heteroestruturas minerais bidimensionais de talco e grafita", In: *3° Encontro dos Pesquisadores de Pós-Doutorado do IGc/ USP*, São Paulo, 2021. doi: https://doi.org/10.5281/zenodo.5720722.

[11] NOBRE, A.G., SALAZAR-NARANJO, A.F., ANDRADE, F.R.D., *et al.*, "Laboratory simulation of talc and graphite geological heterostructures by end-loaded piston-cylinder apparatus", In: *9° Congresso Brasileiro de Carbono*, pp. 144, São Paulo, 2021.

[12] GEIM, A.K., NOVOSELOV, K.S., "The rise of graphene", *Nanoscience and Technology: A Collection of Reviews from Nature Journals*, pp. 11–19, 2009. https://doi.org/10.1142/9789814287005_0002.

[13] GEIM, A.K., "Nobel lecture: random walk to graphene", *Reviews of Modern Physics*, v. 83, n. 3, pp. 851–862, 2011. doi: http://dx.doi.org/10.1103/RevModPhys.83.851.

[14] GEIM, A.K., "Graphene: status and prospects", *Science*, v. 324, n. 5934, pp. 1530–1534, 2009. doi: http://dx.doi.org/10.1126/science.1158877. PubMed PMID: 19541989.

[15] NOBRE, A.G., SILVA, L.P.N., ANDRADE, F.R.D. "Graphene geology and the fourth industrial revolution", In: Iano, Y., Saotome, O., Vásquez, G.L.K., Pezzuto, C.C., Gomes de Oliveira, G. (eds), Smart Innovation, Systems and Technologies, 1 ed., chapter 34, Cham, Switzerland, Springer Nature, 2022. doi: https://doi.org/10.1007/978-3-031-04435-9_34.

[16] FRISENDA, R., NIU, Y., GANT, P., *et al.*, "Naturally occurring van der Waals materials", *2D Materials and Applications*, v. 4, n. 1, pp. 1–13, 2020. doi: https://doi.org/10.1038/s41699-020-00172-2.

[17] ČAPKOVÁ, P., MATĚJKA, V., TOKARSKÝ, J., *et al.*, "Electrically conductive aluminosilicate/graphene nanocomposite", *Journal of the European Ceramic Society*, v. 34, n. 12, pp. 3111–3117, 2014. doi: http://dx.doi.org/10.1016/j.jeurceramsoc.2014.03.021.

[18] ALENCAR, A.B., BARBOZA, A.P.M., ARCHANJO, B.S., *et al.*, "Experimental and theoretical investigations of monolayer and few-layer talc", *2D Materials*, v. 2, n. 1, pp. 1–8, 2015. doi: https://doi.org/10.1088/2053-1583/2/1/015004

[19] MANIA, E., ALENCAR, A.B., CADORE, A.R., *et al.*, "Spontaneous doping on high quality talc-graphene-hBN van der Waals heterostructures", *2D Materials*, v. 4, n. 3, pp. 1–13, 2017. doi: https://doi.org/10.1088/2053-1583/aa76f4

[20] SZABÓ, G.A.J., ANDRADE, F.R.D., GUIMARÃES, G.B., *et al.*, "As jazidas de talco no contexto da história metamórfica dos metadolomitos do Grupo Itaiacoca, PR", *Geologia USP. Série Científica*, v. 5, n. 2, pp. 13–31, 2006. doi: http://dx.doi.org/10.5327/S1519-874X2006000100002.

[21] SAUNITE, D.M., BELLO, R.M.S., ANDRADE, F.R.D., *et al.*, "Metadolomitos talcificados do Grupo Itaiacoca, Paraná: regime de fluidos e implicações genéticas", *Geologia USP. Série Científica*, v. 11, n. 1, pp. 171–187, 2011. doi: http://dx.doi.org/10.5327/Z1519-874X2011000100010.

[22] PRAZERES FILHO, H.J., HARARA, O.M., BASEI, M.A.S., *et al.*, "Litoquímica, geocronologia U-Pb e Geologia isotópica (Sr-Nd-Pb) das rochas graníticas dos batólitos Cunhaporanga e Três Córregos na porção sul do Cinturão Ribeira, Estado do Paraná", *Geologia USP. Série Científica*, v. 3, n. 1, pp. 51–70, 2003. doi: http://dx.doi.org/10.5327/S1519-874X2003000100005.

[23] BOYD, F.R., ENGLAND, J.L., "Apparatus for phase-equilibrium measurements at pressures up to 50 kilobars and temperatures up to 1750°C", *Journal of Geophysical Research*, v. 65, n. 2, pp. 741–748, 1960. doi: http://dx.doi.org/10.1029/JZ065i002p00741.

[24] HOLLOWAY, J.R., WOOD, B.J., *Simulating the Earth: experimental geochemistry*, 1 ed., London, Springer Science & Business Media, 2012.

[25] MCDADE, P., WOOD, B.J., VAN WESTRENEN, W., *et al.*, "Pressure corrections for a selection of piston-cylinder cell assemblies", *Mineralogical Magazine*, v. 66, n. 6, pp. 1021–1028, 2002. doi: http://dx.doi.org/10.1180/0026461026660074.

[26] VLACH, S.R.F., SALAZAR-NARANJO, A.F., TORRES-CORREDOR, J.S., *et al.*, "Calibration of high-temperature furnace assemblies for experiments between 200 and 600 MPa with end-loaded piston-cylinder apparatuses", *Brazilian Journal of Geology*, v. 49, n. 1, pp. 1–7, 2019. doi: http://dx.doi.org/10.1590/2317-488920192018090.

[27] PAWLEY, A.R., WOOD, B.J., "The high-pressure stability of talc and 10 Å phase: potential storage sites for H2O in subduction zones", *The American Mineralogist*, v. 9, n. 9–10, pp. 998–1003, 1995. doi: http://dx.doi.org/10.2138/am-1995-9-1015.

[28] OGANOV, A.R., HEMLEY, R.J., HAZEN, R.M., *et al.*, "Structure, bonding, and mineralogy of carbon at extreme conditions", *Reviews in Mineralogy and Geochemistry*, v. 75, n. 1, pp. 47–77, 2013. doi: http://dx.doi.org/10.2138/rmg.2013.75.3.

[29] TUINSTRA, F., KOENIG, J.L., "Raman spectrum of graphite", *The Journal of Chemical Physics*, v. 53, n. 3, pp. 1126–1130, 1970. doi: http://dx.doi.org/10.1063/1.1674108.

[30] FERRARI, A.C., MEYER, J.C., SCARDACI, V., *et al.*, "Raman spectrum of graphene and graphene layers", *Physical Review Letters*, v. 97, n. 18, pp. 187401, 2006. doi: http://dx.doi.org/10.1103/PhysRevLett.97.187401. PubMed PMID: 17155573.

[31] FERRARI, A.C., "Raman spectroscopy of graphene and graphite: disorder, electron–phonon coupling, doping and nonadiabatic effects", *Solid State Communications*, v. 143, n. 1–2, pp. 47–57, 2007. doi: http://dx.doi.org/10.1016/j.ssc.2007.03.052.

[32] SINGH, V., JOUNG, D., ZHAI, L., *et al.*, "Graphene based materials: past, present and future", *Progress in Materials Science*, v. 56, n. 8, pp. 1178–1271, 2011. doi: http://dx.doi.org/10.1016/j.pmatsci.2011.03.003.

[33] KLEIN, C., DUTROW, B., *Manual of mineral science*, 23 ed., New Jersey, John Wiley & Sons, 2008.

[34] RANTITSCH, G., LÄMMERER, W., FISSLTHALER, E., *et al.*, "On the discrimination of semi-graphite and graphite by Raman spectroscopy", *International Journal of Coal Geology*, v. 159, pp. 48–56, 2016. doi: http://dx.doi.org/10.1016/j.coal.2016.04.001.

[35] REYNARD, B., BEZACIER, L., CARACAS, R., "Serpentines, talc, chlorites, and their high-pressure phase transitions: a Raman spectroscopic study", *Physics and Chemistry of Minerals*, v. 42, n. 8, pp. 641–649, 2015. doi: http://dx.doi.org/10.1007/s00269-015-0750-0.